Electronic Supplementary Material (ESI) for Journal of Materials Chemistry A.

Supporting Information

Bimetallic Metal-Organic Framework-Derived MoFe-PC Microspheres toward Highly Efficient Electrocatalytic Ammonia Synthesis under Ambient Conditions

Silong Chen,‡[a] Haeseong Jang,‡[b] Jia Wang,[a] Qing Qin,*[a] Xien Liu,*[a] and Jaephil Cho*[b]

[a]State Key Laboratory Base of Eco-Chemical Engineering, College of Chemical Engineering, College of Chemistry and Molecular Engineering, Qingdao University of Science and Technology, Qingdao, 266042, P. R. China

[b]Department of Energy Engineering and School of Energy and Chemical Engineering, Ulsan National Institute of Science and Technology (UNIST), Ulsan 689-798, South Korea

List of contents

1. Chemicals

2. Materials Synthesis

3. Materials Characterization

4. Cathode preparation

5. Electrochemical NRR measurements

Figure S1. a) XRD patterns of the Mo-MOF, Fe-MOF and MoFe-MOF. b) SEM image of the MoFe-MOF. c) SEM image of MoFe-PC microspheres derived from MoFe-MOF.

Figure S2. The comparison of XRD patterns of MoFe-MOF with Mo-MOF, and Fe-MOF.

Figure S3. TEM image of the MoFe-PC microspheres.

Figure S4. The XRD patterns of the MoFe-PC (red) and MoFe-MOF (black).

Figure S5. Element linear distributions of Fe, Mo, O, P, and C.

Figure S6. High resolution XPS spectra of O 1s before and after NRR testing.

Figure S7. a) XANES spectra for Fe K-edge of Fe foil, FeO, Fe_2O_3, Fe_3O_4, and MoFe-PC. b) The k^2-weighted Fourier transform of EXAFS spectra for Fe K-edge of Fe foil, FeO, Fe_2O_3, Fe_3O_4, and MoFe-PC. c) XANES spectra for Mo K-edge of Mo foil, MoO_2, MoO_3, and MoFe-PC. d) The k^2-weighted Fourier transform of EXAFS spectra for Mo K-edge of Mo foil, MoO_2, MoO_3, and MoFe-PC.

Figure S8. The linear sweep voltammetry (LSV) curves of MoFe-PC microspheres in N_2- and Ar-saturated 0.1 M HCl solution.

Figure S9. a) UV-Vis absorption spectra of indophenol assays with NH_4^+ after incubated for 2 h at room temperature. b) Calibration curve used for estimation of NH_4Cl.

Figure S10. a) UV-Vis curves of various $N_2H_4 \cdot H_2O$ concentration after incubated for 2 h in 0.1 M HCl electrolyte at room temperature. b) calibration curve used for estimation of $N_2H_4 \cdot H_2O$ concentration. c) UV-Vis absorption spectra of the 0.1 M HCl electrolyte stained with $N_2H_4 \cdot H_2O$ color agent before and after 1 h electrolysis at -0.15 V vs RHE.

Figure S11. Long-time chronoamperometry curve of MoFe-PC catalyst at -0. 5 V vs RHE.

Figure S12. Recycling test of NH_3 yields and Faradaic efficiencies over MoFe-PC electrodes for five times at potential of -0.5 V (vs. RHE).

Figure S13. UV-Vis absorption spectra of the 0.1 M HCl electrolytes colored with indophenol indicator after charging at -0. 5 V for 1 h under different conditions.

Figure S14. UV-Vis absorption spectra of the 0.1 M HCl electrolyte stained with NH_3 color agent before and after 1 h electrolysis at -0.5 V vs. RHE in N_2 atmosphere.

Figure S15. UV-Vis absorption spectra of the 0.1 M HCl electrolyte stained with NH_3 color agent before and after 1 h electrolysis at -0.5 V vs. RHE in Ar atmosphere.

Figure S16. UV-Vis absorption spectra of the 0.1 M HCl electrolyte stained with NH_3 color agent before and after 1 h electrolysis at -0.5 V vs. RHE in N_2 atmosphere on the MoFe-PC electrode at open-circuit potential under ambient conditions.

Figure S17. UV-Vis absorption spectra of the 0.1 M HCl electrolyte stained with NH_3 color agent before and after 1 h electrolysis at -0.5 V vs. RHE without N_2 supplying.

Figure S18. The transection image of MoFe-PC microspheres.

Figure S19. Characterizations of the catalyst collected after the continuous NRR testing for 24 h. a) SEM image, b) TEM image.

Table S1. ICP analysis of Mo and Fe in the electrolyte

Table S2. Comparison of the NRR performance of the MoFe-PC catalyst with other recently reported catalysts in acidic electrolyte

Chemicals

$MoCl_5$, $FeCl_3·6H_2O$, 2,5-dihydroxyterephthalic acid, $NaH_2PO_2·H_2O$, and ethanol were purchased from J&K Scientific LTD. All the chemicals were used without further purification.

Materials Synthesis

Synthesis of MOF-derived FeMo-PC microspheres: In a typical procedure, 0.25 g of $MoCl_5$ and 0.25 g of $FeCl_3·6H_2O$ were added into 15 mL of ethanol to form a homogenous solution under vigorously stirring. Meanwhile, 0.35 g of 2,5-dihydroxyterephthalic acid was dissolved in 20 mL of ethanol. Then, the above two solutions were mixed and the resultant dark brown mixture was transferred into a 50 mL of stainless-steel autoclave, sealed and heated to 170 ^oC for 36 h. After cooling to room temperature naturally, the dark grey products were fully washed with ethanol and then dried in a vacuum oven at 60 ^oC for 6 h.

2.00 g of $NaH_2PO_2·H_2O$ was added to a combustion boat that was placed at the upstream of the tubular furnace. Then, 40 mg of the above dark grey solid powder ($m_{NaH2PO2·H2O}$: $m_{solid\ powder}$ = 50 : 1) was added into another combustion boat, which was placed at the downstream of the tubular furnace. The two combustion boats were wrapped by tinfoil. After outgassed, the tubular furnace was heated to 300 ^oC with a heating rate of 2 ^oC /min and maintained for 2 h under an Ar flow. When the reaction was over, the black products were collected and directly used for the electrochemical tests.

Synthesis of MOF-derived FeMo-C microspheres: The synthetic method of FeMo-C was similar with that of FeMo-PC, except that the $NaH_2PO_2·H_2O$ was not added to the reaction system at the annealing step.

Materials Characterization

The structure and the composition of the prepared catalysts were carefully measured by XRD, SEM, TEM, HRTEM, XPS, XANES, and EXAFS. The XRD measurements were carried out on a Bruker D8 Focus Diffraction system with Cu Kα radiation. A JSM-7500F field-emission scanning electron microscope (FESEM) was used to observe the morphology of the catalysts. TEM and HRTEM measurements were performed on a Tecnai G20 transmission electron microscope at an accelerating voltage of 120 kV. The XPS spectra were calibrated against the carbon 1s photoelectron signal at 284.5 eV on a K-Alpha Analytical instrument. Fe/Mo K-edge X-ray absorption spectra, X-ray absorption near edge structure (XANES) spectra, and extended EXAFS spectra were tested on the BL10C beam line using the Pohang Light Source (PLS-II) in Korea with top-up mode operation under a ring current of 200 mA at 3.0 G eV.

Cathode preparation

Typically, 3 mg of the as-synthesized catalyst was added to a mixed solution composed of 0.15 mL of ethanol and 0.075 mL of ultrapure water. Then, 30 μL of Nafion (5 wt %) solution was added to the above solution. After ultrasonic treatment for 20 min, 20 μL of the homogeneous catalyst ink was dropped on a fluorine doped tin dioxide conductive glass (FTO) with an area of 2 × 1 cm^2 and dried under the ambient condition. The catalyst loading is 0.2 mg.

Electrochemical NRR measurements

All the electrochemical experiments were carried out at room temperature in a typical H-type cell separated by a Nafion 117 membrane. 0.1 M HCl solution was used as the electrolyte. Before N_2 reduction testing, the Nafion membrane was firstly placed in a 5 wt% H_2O_2 aqueous solution and heated to 80 ^oC for 1 h, and then heated to 80 ^oC for another 1 h in ultrapure water. The NRR tests were performed in a three-electrode system with FTO conductive glass coated with catalysts as the working electrode, an Ag/AgCl electrode as the reference electrode and a graphite rod as the counter electrode. All the potentials were calibrated to reversible hydrogen electrode (RHE) according to the following formula: E (vs RHE) = $E_{Ag/AgCl}$ + 0.197 + 0.059 × pH. All polarization curves were steady-state ones after several cyclic voltammetry cycles. Before each NRR measurement, the electrolyte was purged with N_2 for 30 min. The highly pure N_2 was continuously fed to the cathodic compartment using properly positioned spargers during the NRR testing. The potentiostatic tests in 0.1 M Ar-saturated HCl electrolyte were also conducted for comparison. In order to verify that the NH_3 is produced from the electrocatalytic NRR testing, a series of controlling experiments, including the potentiostatic tests at an open-circuit with stable N_2 supplying, or at no applied potential with N_2 supplying, or using the bare FTO as the working electrode, were carried out.

Determination of NH_3:

The production of NH_3 was determined by UV-vis spectrophotometry with indophenol blue method. In detail, 2 mL aliquot of the electrolyte after potentiostatic test was mixed with 2 mL of a 1 m NaOH solution composed of 5 wt% sodium citrate and 5 wt% salicylic acid. Then, 1 mL of 0.05 M NaClO solution and 0.2 mL of 1 wt% $C_5FeN_6Na_2O$ (sodium nitroferricyanide) were sequentially added. After standing for 2 h at room temperature, the mixed solution was measured by an UV-vis spectrophotometer at a wavelength of 655 nm. To accurately quantify NH_3, a calibration curve about linear relation between the absorbance value with NH_3 concentration was obtained by preparing a series of ammonium chloride standard solutions. The formation rate of NH_3 by NRR was calculated based on the equation as follows:

NH_3 Yield Rate = $c_{NH4Cl} \times 0.318 \times V / (t \times m)$.

Where c_{NH4Cl} is the measured NH_4Cl concentration, V is the volume of electrolyte, t is the reduction reaction time, m is the catalyst loading.

Determination of Faradaic Efficiency (FE):

Assuming a three-electron process for NRR, the FE in 0.1 M HCl solution was calculated according to the following equation:

$FE = 3F \times c_{NH4Cl} \times 0.318 \times V / (17 \times Q)$

Where F is the Faraday constant, Q is the quantity of applied electricity.

Determination of hydrazine:

The hydrazine produced in the electrochemical testing was detected by Watt and Chrisp method with 5.99 g of para-(dimenthylamino) benzaldehyde, 30 mL of HCl (concentrated) and 300 mL of ethanol as the color agent. A calibration curve was plotted by preparing a serious of hydrazine monohydrate standard solutions.

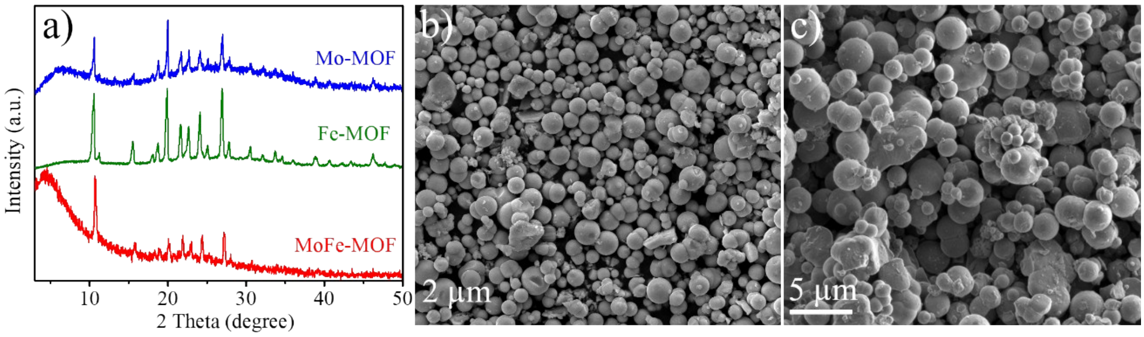

Figure S1. a) XRD patterns of the Mo-MOF, Fe-MOF and MoFe-MOF. b) SEM image of the MoFe-MOF. c) SEM image of MoFe-PC microspheres derived from MoFe-MOF.

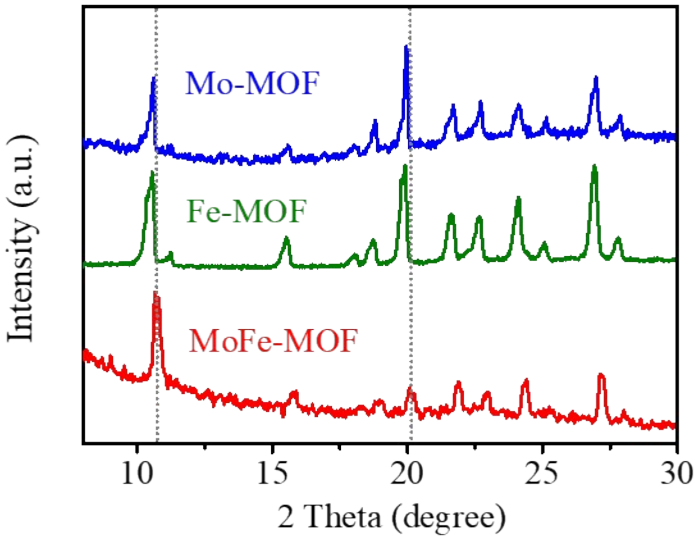

Figure S2. The comparison of XRD patterns of MoFe-MOF with Mo-MOF, and Fe-MOF.

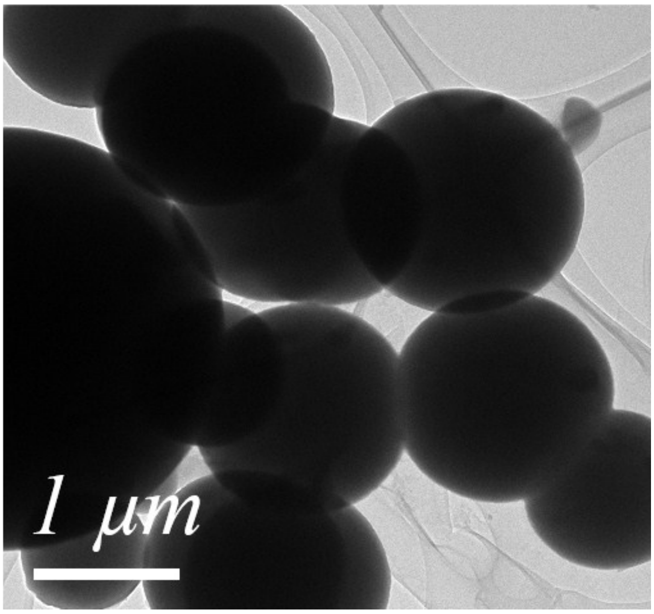

Figure S3. TEM image of the MoFe-PC microspheres.

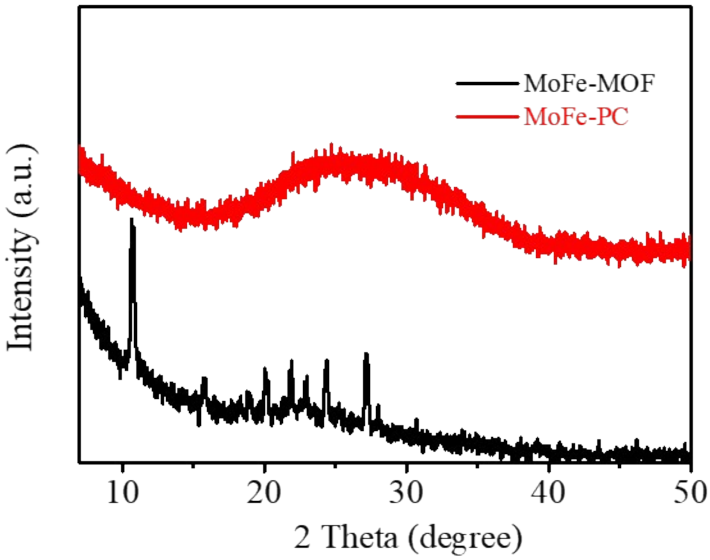

Figure S4. The XRD patterns of the MoFe-PC (red) and MoFe-MOF (black).

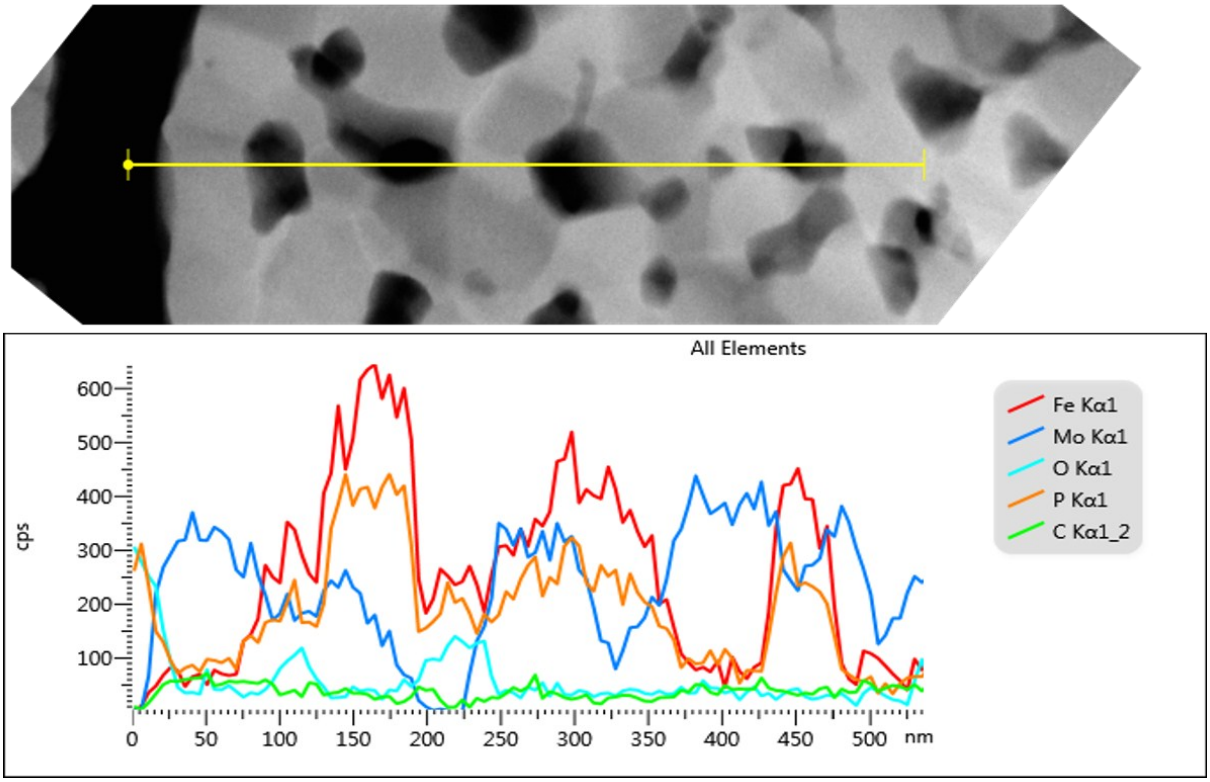

Figure S5. Element linear distributions of Fe, Mo, O, P, and C.

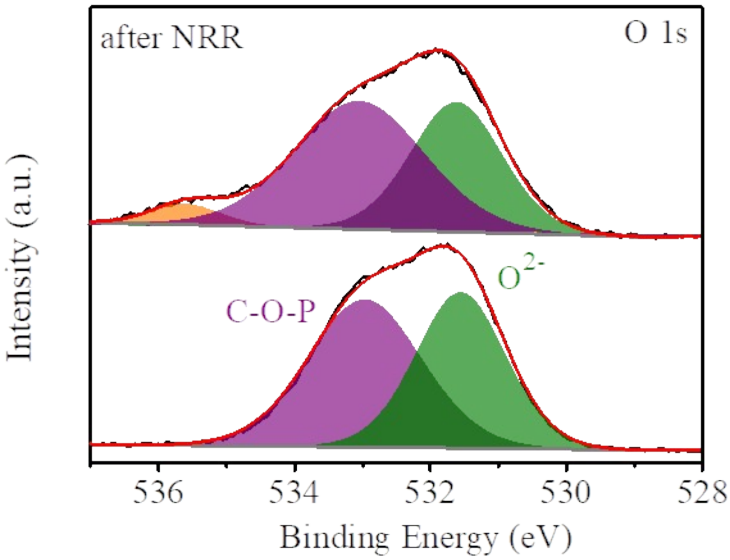

Figure S6. High resolution XPS spectra of O 1s before and after NRR testing.

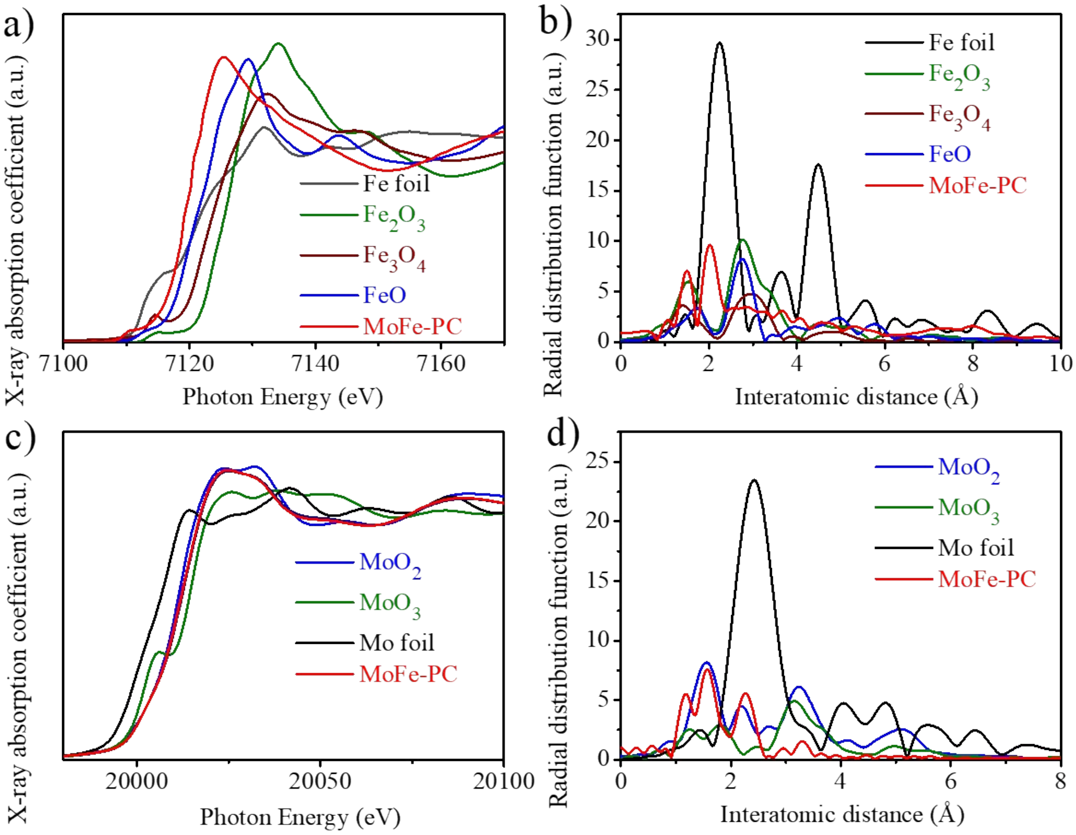

Figure S7. a) XANES spectra for Fe K-edge of Fe foil, FeO, Fe_2O_3, Fe_3O_4, and MoFe-PC. b) The k^2-weighted Fourier transform of EXAFS spectra for Fe K-edge of Fe foil, FeO, Fe_2O_3, Fe_3O_4, and MoFe-PC. c) XANES spectra for Mo K-edge of Mo foil, MoO_2, MoO_3, and MoFe-PC. d) The k^2-weighted Fourier transform of EXAFS spectra for Mo K-edge of Mo foil, MoO_2, MoO_3, and MoFe-PC.

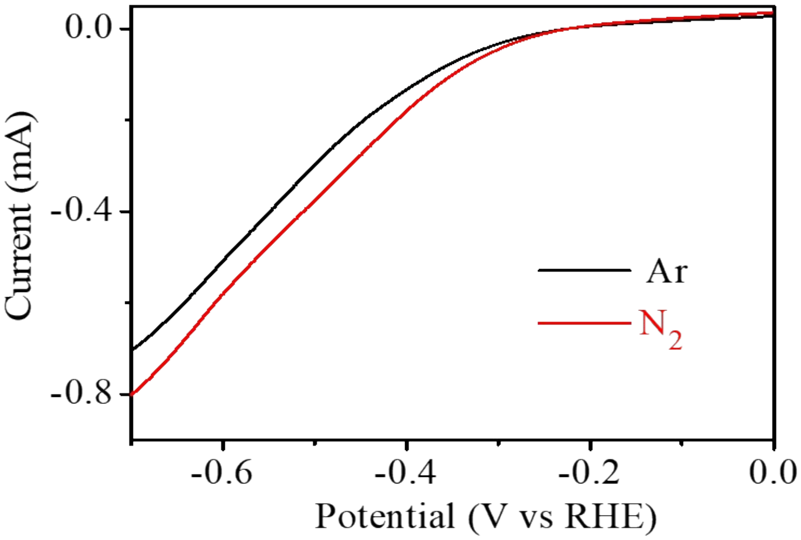

Figure S8. The linear sweep voltammetry (LSV) curves of MoFe-PC microspheres in N_2- and Ar-saturated 0.1 M HCl solution.

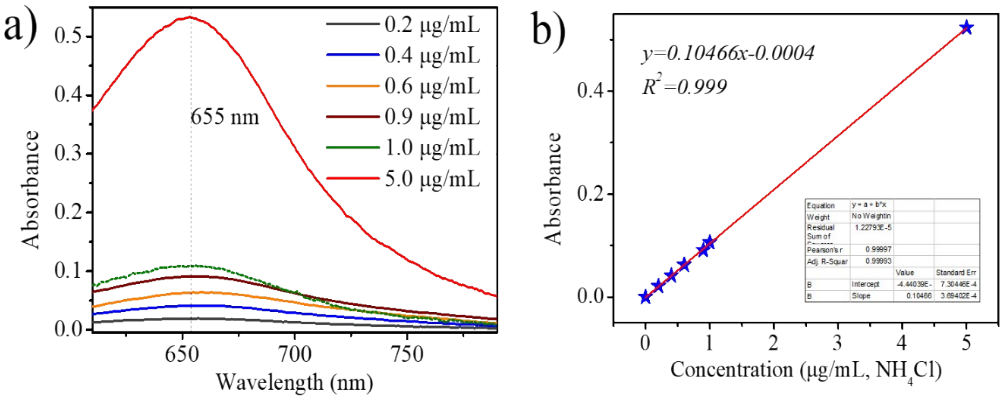

Equation	y = a + b*x		
Weight	No Weightin		
Residual Sum of	1.22793E-5		
Pearson's r	0.99997		
Adj. R-Squar	0.99993		
		Value	Standard Err
B	Intercept	-4.44039E-	7.30446E-4
B	Slope	0.10466	3.69402E-4

Figure S9. a) UV-Vis absorption spectra of indophenol assays with NH_4^+ after incubated for 2 h at room temperature. b) Calibration curve used for estimation of NH_4Cl.

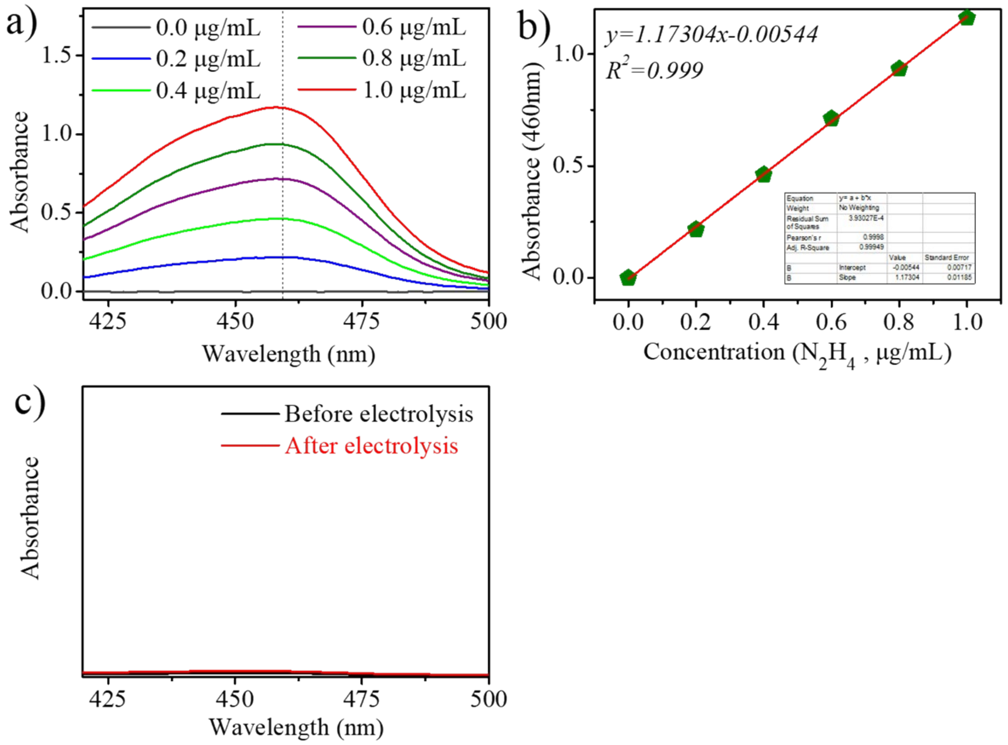

Figure S10. a) UV-Vis curves of various $N_2H_4 \cdot H_2O$ concentration after incubated for 2 h in 0.1 M HCl electrolyte at room temperature. b) calibration curve used for estimation of $N_2H_4 \cdot H_2O$ concentration. c) UV-Vis absorption spectra of the 0.1 M HCl electrolyte stained with $N_2H_4 \cdot H_2O$ color agent before and after 1 h electrolysis at -0.5 V vs RHE.

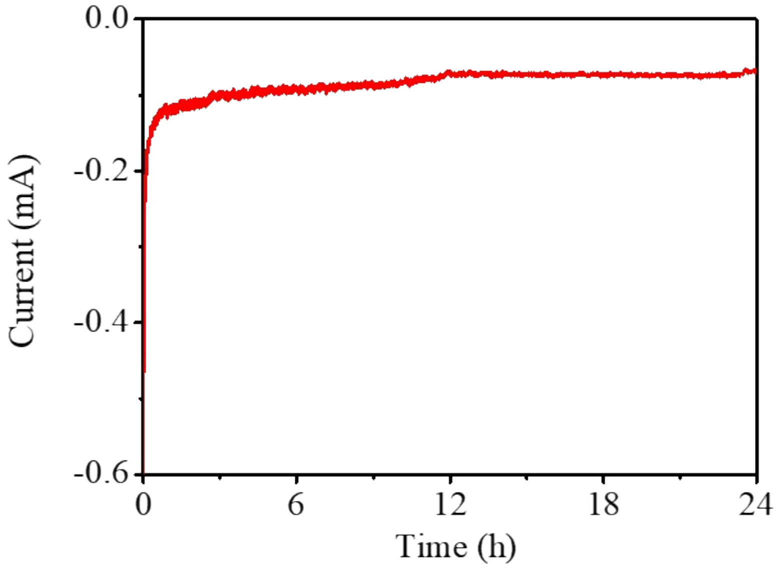

Figure S11. Long-time chronoamperometry curve of MoFe-PC catalyst at -0. 5 V vs RHE.

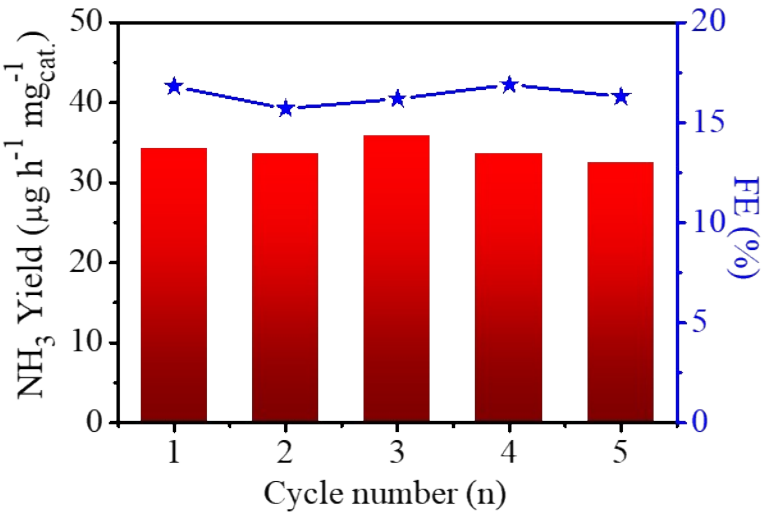

Figure S12. Recycling test of NH_3 yields and Faradaic efficiencies over MoFe-PC electrodes for five times at potential of -0.5 V (vs. RHE).

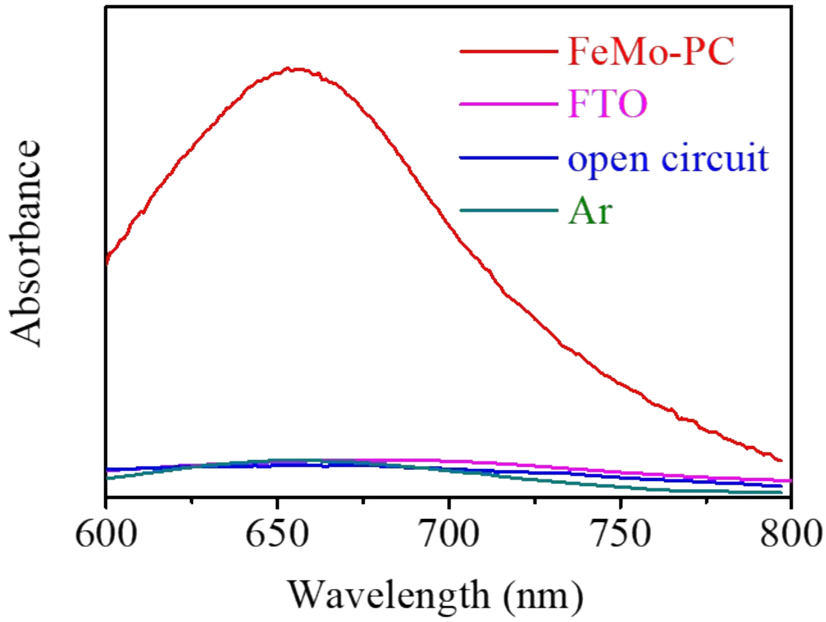

Figure S13. UV-Vis absorption spectra of the 0.1 M HCl electrolytes colored with indophenol indicator after charging at -0. 5 V for 1 h under different conditions.

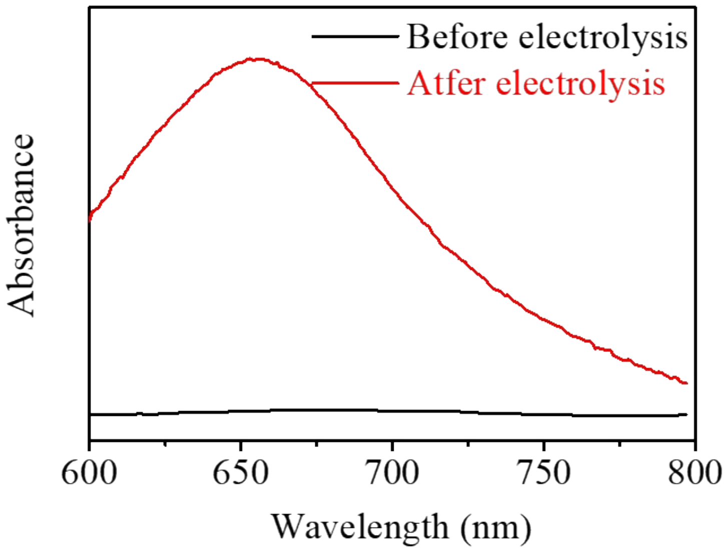

Figure S14. UV-Vis absorption spectra of the 0.1 M HCl electrolyte stained with NH_3 color agent before and after 1 h electrolysis at -0.5 V vs. RHE in N_2 atmosphere.

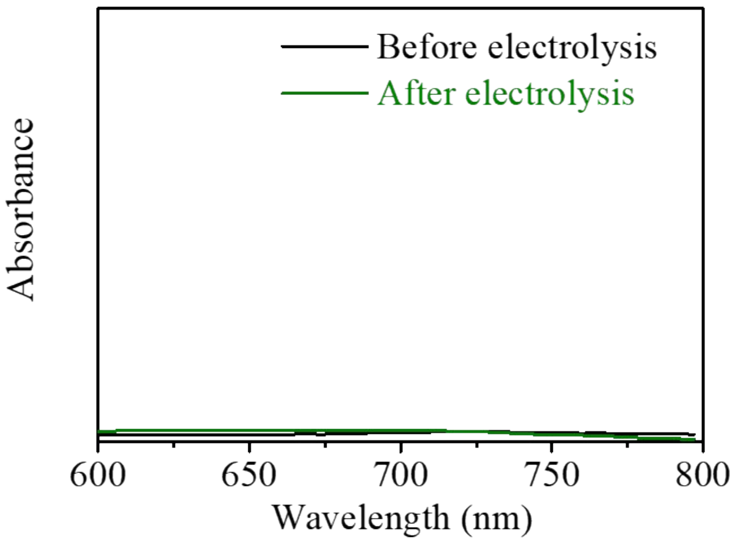

Figure S15. UV-Vis absorption spectra of the 0.1 M HCl electrolyte stained with NH_3 color agent before and after 1 h electrolysis at -0.5 V vs. RHE in Ar atmosphere.

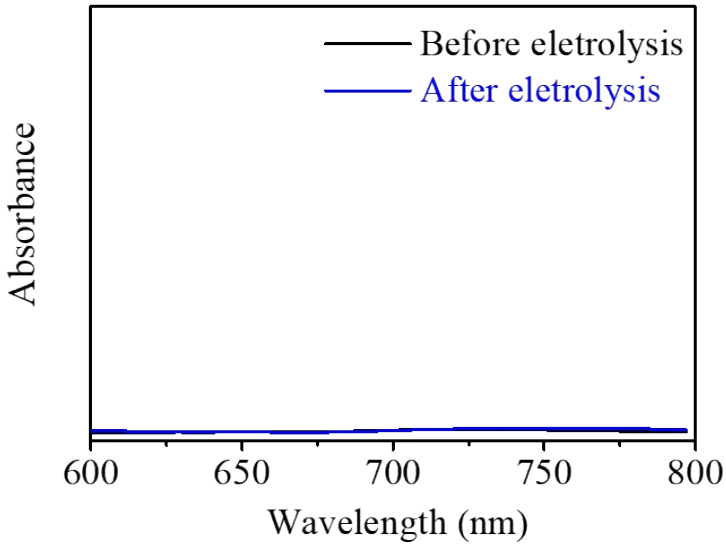

Figure S16. UV-Vis absorption spectra of the 0.1 M HCl electrolyte stained with NH_3 color agent before and after 1 h electrolysis at -0.5 V vs. RHE in N_2 atmosphere on the MoFe-PC electrode at open-circuit potential under ambient conditions.

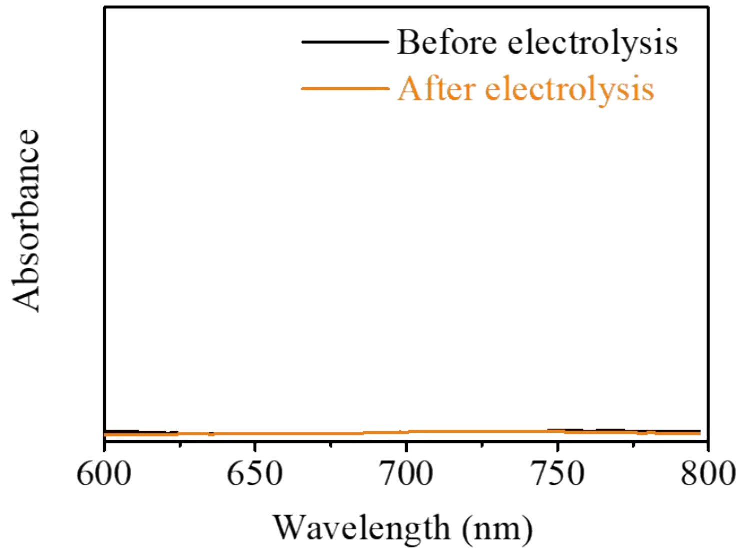

Figure S17. UV-Vis absorption spectra of the 0.1 M HCl electrolyte stained with NH_3 color agent before and after 1 h electrolysis at -0.5 V vs. RHE without N_2 supplying.

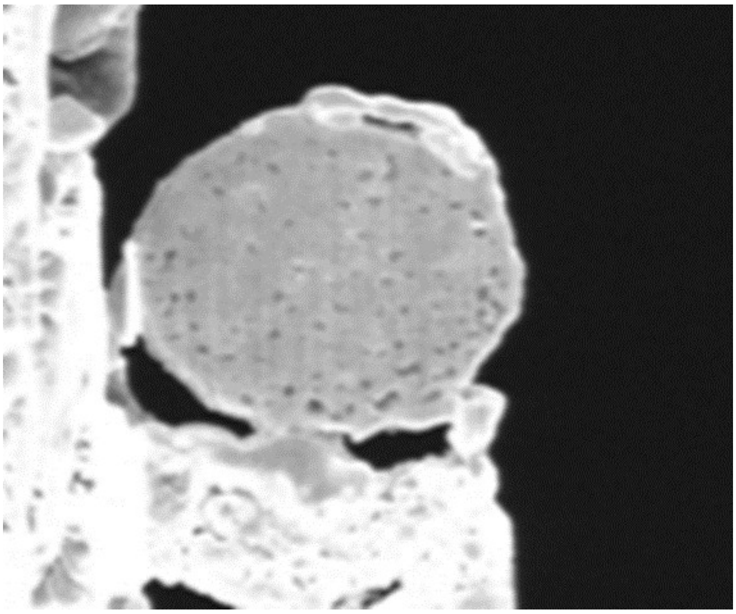

Figure S18. The transection image of MoFe-PC microspheres.

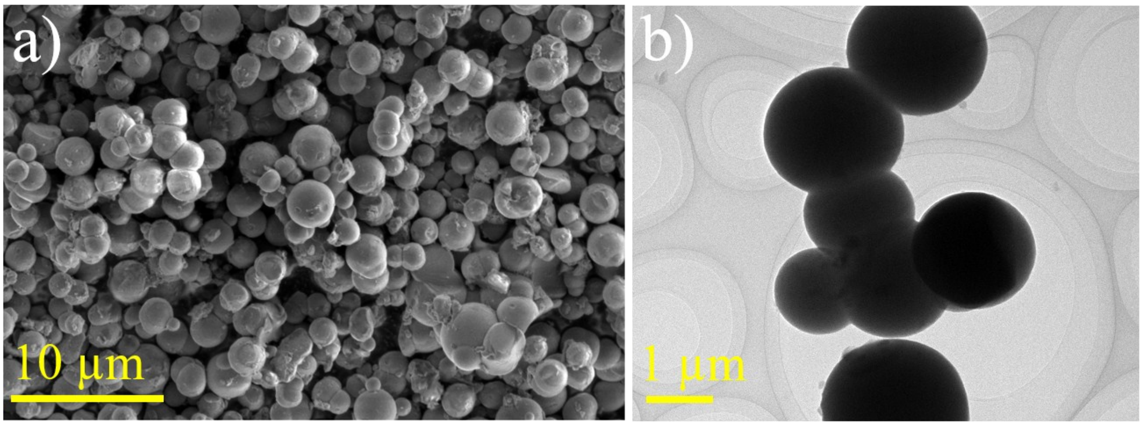

Figure S19. Characterizations of the catalyst collected after the continuous NRR testing for 24 h. a) SEM image, b) TEM image.

Table S1. ICP analysis of Mo and Fe in the electrolyte

Time (min)	**0**	**20**	**40**	**60**
Concentration of Fe (mg/L)	0.006	0.006	0.006	0.006
Concentration of Mo (mg/L)	0.021	0.023	0.022	0.020

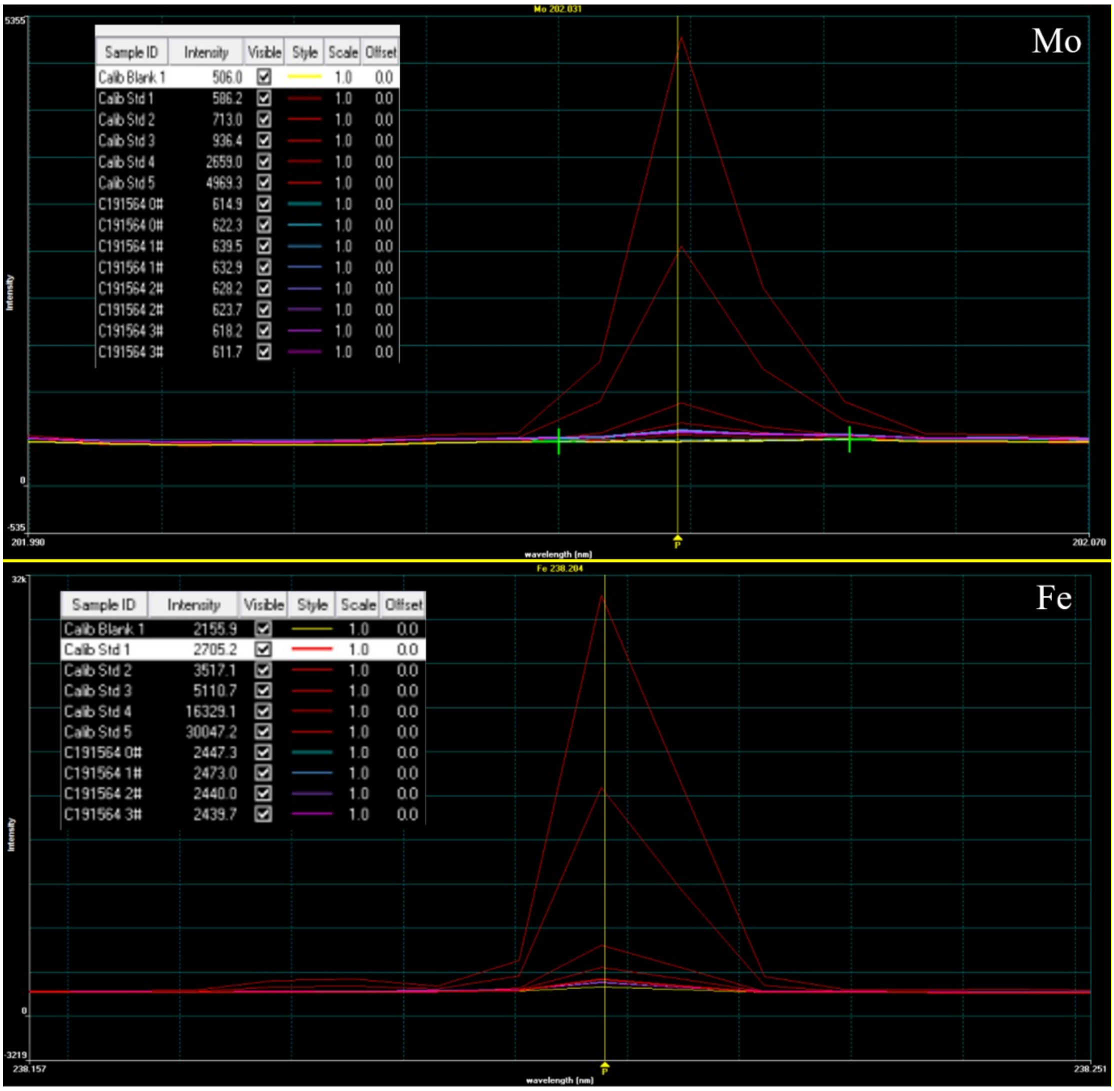

Sample ID	Intensity	Visible	Style	Scale	Offset
Calib Blank 1	506.0	☑	—	1.0	0.0
Calib Std 1	586.2	☑	—	1.0	0.0
Calib Std 2	713.0	☑	—	1.0	0.0
Calib Std 3	936.4	☑	—	1.0	0.0
Calib Std 4	2659.0	☑	—	1.0	0.0
Calib Std 5	4969.3	☑	—	1.0	0.0
C191564 0#	614.9	☑	—	1.0	0.0
C191564 0#	622.3	☑	—	1.0	0.0
C191564 1#	639.5	☑	—	1.0	0.0
C191564 1#	632.9	☑	—	1.0	0.0
C191564 2#	628.2	☑	—	1.0	0.0
C191564 2#	623.7	☑	—	1.0	0.0
C191564 3#	618.2	☑	—	1.0	0.0
C191564 3#	611.7	☑	—	1.0	0.0

Sample ID	Intensity	Visible	Style	Scale	Offset
Calib Blank 1	2155.9	☑	—	1.0	0.0
Calib Std 1	2705.2	☑	—	1.0	0.0
Calib Std 2	3517.1	☑	—	1.0	0.0
Calib Std 3	5110.7	☑	—	1.0	0.0
Calib Std 4	16329.1	☑	—	1.0	0.0
Calib Std 5	30047.2	☑	—	1.0	0.0
C191564 0#	2447.3	☑	—	1.0	0.0
C191564 1#	2473.0	☑	—	1.0	0.0
C191564 2#	2440.0	☑	—	1.0	0.0
C191564 3#	2439.7	☑	—	1.0	0.0

Time-depended ICP-AES measurement is used to detect the concentration of Mo and Fe in the electrolyte. ‘0’ represents that the working electrode is put into the electrolyte and nitrogen bubbles for 20 minutes. After that, the potential is applied for the testing device. We evaluated the concentration of Mo and Fe in the electrolyte each 20 min. According to the ICP-AES analysis results, after bubbling for 20 min, the concentration of Fe and Mo in the electrolyte is 0.006 mg/L and 0.021 mg/L, respectively, which may be due to the falling of the little catalyst off the working electrode caused by bubbling. Afterwards, the concentration of Fe and Mo exhibits no obvious change after continuous electrolysis for 20, 40 and 60 min, respectively. This result demonstrates the high structural stability of the catalyst during the electrochemical process.

Table S2. Comparison of the NRR performance of the MoFe-PC catalyst with other recently reported catalysts in acidic electrolyte

Catalyst	Electrolyte	NH_3 Yield Rate	FE (%)	NH_4^+-N Testing Method	Ref.
MoFe-PC	0.1 M HCl	34.23 μg h^{-1} mg^{-1}	16.83	Indophenol method	Our work
a-Au/CeO_x–RGO	0.1 M HCl	8.3 μg h^{-1} mg^{-1}	10.10	Indophenol method	1
TA-reduced Au/TiO_2	0.1 M HCl	21.4 μg h^{-1} mg^{-1}	8.11	Indophenol method	2
$Bi_4V_2O_{11}$/CeO_2	0.1 M HCl	23.21 μg h^{-1} mg^{-1}	10.16	Indophenol method	3
Mo_2N/GCE	0.1 M HCl	78.4 μg h^{-1} mg^{-1}	4.5	Indophenol method	4
BCN	0.1 M HCl	7.75 μg h^{-1} mg^{-1}	13.79	Indophenol method	5
Au flowers	0.1 M HCl	25.57 μg h^{-1} mg^{-1}	6.05	Indophenol method	6
Ru@ZrO_2/NC	0.1 M HCl	~2.2 μg h^{-1} mg^{-1}	~16	Indophenol method	7
AuSAs-NDPCs	0.1 M HCl	2.32 μg h^{-1} mg^{-1}	12.3	Indophenol method	8
Nb_2O_5/CP	0.1 M HCl	43.6 μg h^{-1} mg^{-1}	9.26	Indophenol method	9
$Ti_3C_2T_x$/CP	0.1 M HCl	20.4 μg h^{-1} mg^{-1}	9.3	Indophenol method	10
B_4C	0.1 M HCl	26.57 μg h^{-1} mg^{-1}	15.95	Indophenol method	11
SA-Mo/NPC	0.1 M HCl	31.5 μg h^{-1} mg^{-1}	6.8	Indophenol method	12

References:

1. Li, S. J.; Bao, D.; Shi, M. M.; Wulan, B. R.; Yan, J. M.; Jiang, Q. Amorphizing of Au Nanoparticles by CeO_x-RGO Hybrid Support towards Highly Efficient Electrocatalyst for N_2 Reduction under Ambient Conditions. *Adv. Mater.* **2017,** *29*, 1700001.

2. Shi, M. M.; Bao, D.; Wulan, B. R.; Li, Y. H.; Zhang, Y. F.; Yan, J. M.; Jiang, Q. Au Sub-Nanoclusters on TiO_2 toward Highly Efficient and Selective Electrocatalyst for N_2 Conversion to NH_3 at Ambient Conditions. *Adv. Mater.* **2017,** *29*, 1606550.

3. Lv, C.; Yan, C.; Chen, G.; Ding, Y.; Sun, J.; Zhou, Y.; Yu, G. An Amorphous Noble-Metal-Free Electrocatalyst that Enables Nitrogen Fixation under Ambient Conditions. *Angew. Chem. Int. Ed.* **2018,** *57*, 6073-6076.

4. Ren, X.; Cui, G.; Chen, L.; Xie, F.; Wei, Q.; Tian, Z.; Sun, X. Electrochemical N_2 fixation to NH_3 under ambient conditions: Mo_2N nanorod as a highly efficient and selective catalyst. *Chem. Commun.* **2018,** *54*, 8474-8477.

5. Chen, C.; Yan, D.; Wang, Y.; Zhou, Y.; Zou, Y.; Li, Y.; Wang, S. BN Pairs Enriched Defective Carbon Nanosheets for Ammonia Synthesis with High Efficiency. *Small* **2019,** *15*, 1805029.

6. Wang, Z.; Li, Y.; Yu, H.; Xu, Y.; Xue, H.; Li, X.; Wang, H.; Wang, L. Ambient Electrochemical Synthesis of Ammonia from Nitrogen and Water Catalyzed by Flower-Like Gold Microstructures. *ChemSusChem* **2018,** *11*, 3480-3485.

7. Tao, H.; Choi, C.; Ding, L.-X.; Jiang, Z.; Han, Z.; Jia, M.; Fan, Q.; Gao, Y.; Wang, H.; Robertson, A. W.; Hong, S.; Jung, Y.; Liu, S.; Sun, Z. Nitrogen Fixation by Ru Single-Atom Electrocatalytic Reduction. *Chem* **2019,** *5*, 204-214.

8. Qin, Q.; Heil, T.; Antonietti, M.; Oschatz, M. Single-Site Gold Catalysts on Hierarchical N-Doped Porous Noble Carbon for Enhanced Electrochemical Reduction of Nitrogen. *Small Methods* **2018,** *2*, 1800202.

9. Han, J.; Liu, Z.; Ma, Y.; Cui, G.; Xie, F.; Wang, F.; Wu, Y.; Gao, S.; Xu, Y.; Sun, X. Ambient N_2 fixation to NH_3 at ambient conditions: Using Nb_2O_5 nanofiber as a high-performance electrocatalyst. *Nano Energy* **2018,** *52*, 264-270.

10. Zhao, J.; Zhang, L.; Xie, X.-Y.; Li, X.; Ma, Y.; Liu, Q.; Fang, W.-H.; Shi, X.; Cui, G.; Sun, X. $Ti_3C_2T_x$ (T = F, OH) MXene nanosheets: conductive 2D catalysts for ambient electrohydrogenation of N_2 to NH_3. *J. Mater. Chem. A* **2018,** *6*, 24031-24035.

11. Qiu, W.; Xie, X. Y.; Qiu, J.; Fang, W. H.; Liang, R.; Ren, X.; Ji, X.; Cui, G.; Asiri, A. M.; Cui, G.; Tang, B.; Sun, X. High-performance artificial nitrogen fixation at ambient conditions using a metal-free electrocatalyst. *Nat. Commun.* **2018,** *9*, 3485.

12. Han, L.; Liu, X.; Chen, J.; Lin, R.; Liu, H.; Lu, F.; Bak, S.; Liang, Z.; Zhao, S.; Stavitski, E.; Luo, J.; Adzic, R. R.; Xin, H. L. Atomically Dispersed Molybdenum Catalysts for Efficient Ambient Nitrogen Fixation. *Angew. Chem. Int. Ed.* **2019,** *58*, 2321-2325.